

# AN INNOVATIVE MODEL FOR CRITICAL HEAT FLUX PREDICTION IN SATURATED POOL BOILING BASED ON BUBBLE BEHAVIORS ON DRY HOT SPOTS

Yuzhao Liu<sup>1</sup>, Yanping Du<sup>1\*</sup>, Shalong Xiong<sup>1</sup>, Tao Zhou<sup>1</sup> and Ziqing Zhao<sup>1</sup>

<sup>1</sup>China-UK Low Carbon College, Shanghai Jiao Tong University, Shanghai, 201306, China

\*Correspondence: yanping.du@sjtu.edu.cn

## ABSTRACT

Ultra-high heat flux cooling has become a research hotspot owing to its wide application in thermal engineering fields. Only by exploring its internal physical mechanism and calculating the CHF (critical heat flux) of different surfaces, can the necessary theoretical basis be provided for the design and optimization of pool boiling heat exchange in engineering applications. Previous models cannot accurately predict CHF value due to the limitations of their physical models. In this paper, a new theoretical physical model was obtained to predict CHF value of pure liquid on a heated surface. The theoretical model proposed a new CHF trigger mechanism based on the bubble behavior near the heater surface. A three-dimensional force balance of a separated bubble was analyzed at CHF condition to derive the analytical correlation for CHF value. The correlation considers the effect of hydraulic pressure, surface tension, liquid properties as well as the contact angle of the heater surface. The predicted values of CHF value on heated surfaces obtained from the present model were found in agreement with existing experimental data within a wide range. It is shown that CHF is mainly affected by factors of adhesion force and hydraulic pressure.

**Keywords:** critical heat flux; pool boiling; bubble behavior; force balance; contact angle

## NONMENCLATURE

<i>Abbreviations</i>	
F	force (N)
g	gravity ( $m/s^2$ )
h	latent heat (J/kg)
H	height (m)
n	bubble diameter effective parameter
L	liquid-vapor contact length (m)
m	mass flow rate (kg/s)
P	pressure ( $N/m^2$ )
$q''$	heat flux ( $W/m^2$ )
R	bubble radius (m)
V	bubble volume ( $m^3$ )
<i>Greek symbols</i>	
$\alpha$	the dynamic receding contact angle
$\beta$	surface orientation
$\sigma$	surface tension (N/m)
$\rho$	density ( $kg/m^3$ )
$\lambda_T$	critical wave length of Taylor instability (m)
<i>Subscripts and superscripts</i>	
a	average
I	interface
l	liquid
M	momentum change due to evaporation (N)
P	hydraulic pressure (N)

S	surface tension at the bubble base (N)
v	vapor
z	along z direction

## 1. INTRODUCTION

As technology evolved, there is a great demand for high heat flux removal in the field of industry like electronic chips [1], photovoltaic [2], Computer data center and Electric vehicles [3]. The extremely high heat flux requires us to develop technology with stronger heat dissipation capacity, since boiling heat transfer takes advantage of latent heat and large heat transfer coefficients as high as  $10^3$ - $10^5$  W/m<sup>2</sup>K. The use of boiling heat transfer for thermal management has received significant interest over the past decades.

However, the key to the application of these techniques is to accurately predict heat transfer performance, especially critical heat flux (CHF). In large area of pool boiling, the CHF is featured as its upper limit for safe operation of thermal systems. A transition from nucleate boiling to film boiling occurs once the CHF has been achieved and the phenomenon of a sharp deduction of heat transfer coefficient appears. The formation mechanisms and influence factors of CHF have been widely investigated and discussed to ensure the safe and reliable operation of thermal management system. In general, fluid properties and surface characters are two major factors affecting the CHF mechanism.

Different predicting methods have been proposed by assuming different trigger mechanisms for CHF based on different understandings of bubble behavior at CHF point. Four models that are widely accepted are categorized as (i) the hydrodynamic instability models, (ii) the hydrodynamic force imbalance model, (iii) the macrolayer dry out models, and (iv) the dry hot spots models.

Kutateladze [4] first proposed the hydrodynamic instability model in 1950, which has been the most recognized model. Many models such as Zuber's model [5], Lienhard and Dhir's model [6] and other semi-empirical models are developed based on Kutateladze's model. These semi-empirical models are used to modify the Zuber's model by fitting the Zuber's model and obtaining additional terms from experimental data. Yagov [7] conducted a comprehensive review of this set of models and found that some of the key hypotheses

could not be proved by experiments or were inconsistent with experimental observation results.

Most of the accurate models [8] used to predict CHF conditions are semi-empirical correlations based on Zuber's model. These models usually contain an empirical fitting function for contact Angle, which is ignored in Zuber's model and Lienhard and Dhir's model. This indicates that the existing hydrodynamic instability model may be an incomplete model, which needs to be modified to more accurately represent experimental observations.

Kandlikar [9] established a CHF prediction model based on the hydrodynamic behavior of a single separated bubble interface. Kandlikar hypothesized that at the inception of CHF, the bubble would extend horizontally and merged with adjacent bubbles to form steam film, and then cover some or all heating surfaces to trigger CHF. Kandlikar considers a two-dimensional force balance of a single large bubble attached to the heater surface, the three-dimensional feature of bubble geometry shape and bubble behavior is not considered, resulting in the low accuracy of this model. However, except for the inaccuracy, this model can provide baseline prediction for a wide range of fluid and operating conditions.

The macrolayer dryout model was first proposed by Haramura and Katto [10]. The macrolayer dryout model assumes that large bubbles are suspended over a macrolayer which contains many small steam jets. The evaporated steam is transported to the large bubbles above through these jets. The model assumes that CHF occurs before bubbles are large enough to escape from the surface and this macrolayer completely evaporates. Thus, CHF can be calculated by the total heat required to evaporate all liquid films in the macrolayer.

Haramura and Katto's model has been modified by many researchers based on different suspension periods and macrolayer thickness models to better fit the experimental data, as described by Fang and Dong [8]. The main uncertainties of this model come from the errors of hover period prediction and macrolayer layer thickness, which are also difficult to measure accurately. The physical processes assumed by the model also contradict many experimental observations, especially those aimed at measuring dry areas beneath bubbles. For example, Chu et al. [11] [12] show that the thick layer has been completely dried when the heat flux is much lower than that of CHF.

The dry hot spot model is proposed by Yagov [13]; it is observed through experiments that the dry hot spot

area fraction increases with the increase of heat flux in pool boiling. The dry spot theory predicts CHF values based on the fact that CHF occurs when liquids cannot rewet the growing hot spots. Dry hot spots can be reversible or irreversible. If rewetting occurs as the bubbles leave the surface, the hot spots are reversible. Otherwise, the hot spots are irreversible. The CHF condition is initiated when Irreversible Hot Spot (IHS) increases over time and permanently covers a substantial portion or even the whole heating surface. According to Zhao et al. [14], the proposed IHS model can predict the CHF on both small flat surfaces and long horizontal cylinders within 5% uncertainty by using the actual heating surface area.

In this regard, an innovative theoretical model is developed in this paper with a comprehensive consideration of three dimensional forces including the hydraulic pressure, adhesion force, gravity, and force caused by the vapor momentum change. This model modifies the bubble diameter based on Kandlikar's assumptions, and combines the force imbalance model as well as the dry hot spot model. Through force imbalance analysis of bubbles over dry hot spots, the obtained correlation improved the accuracy of the prediction as well as broadened the application range. It is worth mentioning that the hydraulic pressure can be quantitatively determined based on the established model. Furthermore, the factors such as the liquid height and the bubble size that affect the variation of the hydraulic pressure are evaluated in details.

## 2. PROCESS ANALYSIS

The critical heat flux (CHF) represents the safe operational limit in a two-phase boiling heat transfer system, marking the point when a vapor film begins to cover the heated surface, and the heater surface starts to dry out. After CHF, the heater surface will be covered by thin vapor film which deteriorates the steam removal process, and the heat flux decreases with the increment of the wall superheat.

As the heat flux is applied on the surface, a few bubbles start to emerge and the coefficient of heat transfer increases sharply due to the consistent departure of bubbles. As shown in Figure 1, just before the inception of CHF condition, those separated bubbles will expand and form a large coalesced bubble; the large bubble will then depart and leave a few separated bubbles over the surface. These separated bubbles gradually coalesce together and form a thin vapor film

over the heater surface, which causes the CHF condition to occur.

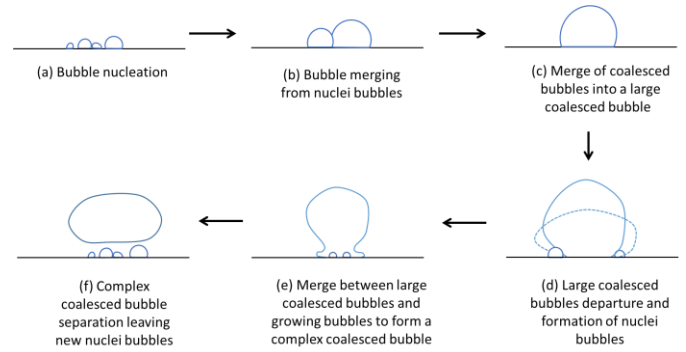


Figure. 1 The two-dimensional periodic behaviour of bubbles on a smooth surface before the inception of CHF condition.

## 3. CHF MODEL FOR SMOOTH SURFACE

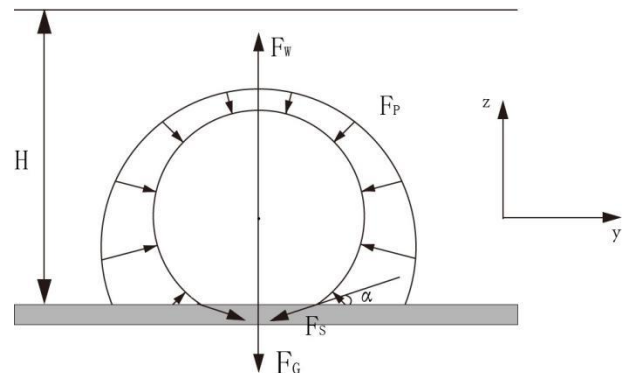


Figure. 2 Force balance of a boiling bubble on smooth heated surface.

We now analyze a separated bubble attached on the heater surface during boiling process near CHF condition. Figure 1 is a schematic diagram of a bubble attached to a horizontal heated surface. The bubble is assumed to be in spherical shape, according to symmetry principle, the forces acting on it can be simplified to the direction normal to the heated surface. The force balance of the bubble can be analyzed at the z direction. The bubble is governed by forces including the surface adhesion force, the hydraulic pressure, the gravity, and the inertia force. The surface adhesion force  $F_s$  acts along the liquid-solid interface at the bubble base. The liquid surface plane has a height over the top of the bubble surface. It results in an increased pressure distribution exerted on the bubble surface. The hydraulic pressure  $F_p$  acts normal to the bubble surface, pointing to the center of the sphere. At the CHF

point, it is assumed that within the bubble region the heating surface is dried out, so there is no hydraulic pressure acting at the bubble base. The gravity of the vapor inside of the bubble region is also taken into consideration as  $F_G$ . With high evaporation rates approaching the CHF condition, vapor is continuously generated inside the bubble, which enables the bubble interface to propagate with a high velocity. The change in momentum caused by evaporation can be expressed as  $F_M$ , which acts uniformly to the bubble surface. A detailed three-dimensional force balance is performed below to obtain the CHF in the given condition.

Assuming that bubble has a uniform radius of  $R$  and the surface tension force acts at the base of the bubble, the length over which the force acts is given by:

$$L = 2\pi R \sin \alpha \quad (1)$$

In which  $\alpha$  is the dynamic contact angle of the liquid-vapor interface with the solid heater surface. The surface tension force  $F_S$  is given by:

$$F_S = -L\sigma \quad (2)$$

Where  $\sigma$  represents the surface tension, N/m.

Kandlikar assumes the average bubble size can be taken as  $\lambda_T/2$ . The critical wavelength for initiating this instability is given by Zuber:

$$\lambda_T = C_1 2\pi \left[ \frac{\sigma}{g(\rho_l - \rho_v)} \right]^{1/2} \quad (3)$$

The value of  $C_1$  ranges from 1 to  $\sqrt{3}$ . With  $C_1 = 1$ , average bubble radius  $R_a$  can be obtained:

$$R_a = \frac{1}{2} \pi \left[ \frac{\sigma}{g(\rho_l - \rho_v)} \right]^{1/2} \quad (4)$$

The Kandlikar's CHF model analyzes the dynamic behavior of the bubbles and suggests that as the bubbles start to be stretched sideways when they grow to a given size (i.e.  $\lambda_T/2$ ). The selection of bubble size is based on the average bubble diameter, but in experimental research, there is no direct evidence showing this situation. By applying force balance analysis on a bubble, it is easy to find out that on hydrophilic surface, this average diameter is too large for the bubble to stay on the surface. The time-averaged bubble diameter cannot represent the actual boiling situation, especially with the change of contact

angle of the heater surface. Costello and Frea [15], Fong et al. [16] said small contact angle is conducive to the liquid flow into the bubble base, which assists bubble departure and leads to a smaller bubble departure diameter. To fit the experimental CHF results, the effective parameter was multiplied by the diameter value. The bubble diameter can be further corrected considering contact angle:

$$R = \frac{1}{2} \pi \left[ \frac{\sigma \sin^n \alpha}{g(\rho_l - \rho_v)} \right]^{1/2} \quad (5)$$

Where  $n$  is the effective parameter, and is recommended to be 2.8.

The bubble volume  $V$  is given by:

$$V = \frac{\pi R^3}{3} (2 + 3 \cos \alpha - \cos^3 \alpha) \quad (6)$$

The force  $F_G$  is due to gravity of the vapor:

$$F_G = -\rho_v V g \quad (7)$$

For simplification of the calculation, a spherical coordinate is established with its origin aligned to the bubble center. The bubble is subjected to a pressure field  $P$  that linearly increases with the change of the liquid depth, which is described as below:

$$P = \rho_l g (H - R \cos \alpha - z) \quad (8)$$

The hydraulic pressure acts over the surface of a semi spherical bubble, the resultant force along the  $z$  direction  $F'_{Pz}$  can be calculated under spherical coordinates:

$$\begin{aligned} F'_{Pz} &= - \int_0^{2\pi} \int_0^{\pi-\alpha} [\rho_l g (H - R \cos \alpha - R \cos \theta)] R^2 \sin \theta d\theta d\phi \cos \theta \\ &= 2\pi \rho_l g R^2 \left[ \frac{1}{4} (H - R \cos \alpha) (\cos 2\alpha - 1) + \frac{1}{3} R (\cos^3 \alpha + 1) \right] \end{aligned} \quad (9)$$

$F'_{Pz}$  represents the static pressure acting on the bubble. However, in real boiling process, the liquid around the bubble is in turbulent state and flows with certain velocity. Therefore, a dynamic pressure will act on the bubble, causing certain reduction to the static pressure. To illustrate this effect, the pressure on the bubble can be expressed as  $\varphi F'_{Pz}$  regarding experimental results.

$$F_{Pz} = \varphi F'_{Pz} \quad (10)$$

In which  $\varphi$  is the pressure effective parameter, and is recommended to be 0.66.

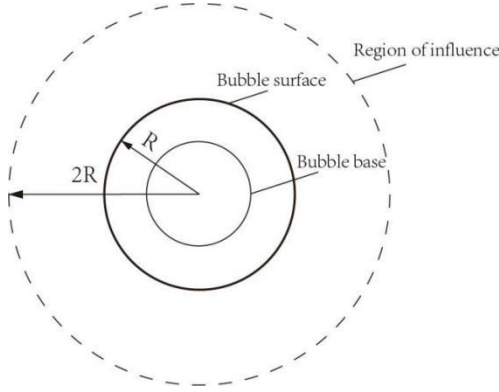


Figure. 3 Sketch showing region of influence, bubble diameter, and bubble base size.

Heat is removed by the bubble from the bubble surface area  $S$ :

$$S = 2\pi R^2 (1 + \cos \alpha) \quad (11)$$

The heat flux due to evaporation per unit area of the interface is expressed as  $q_I''$ , and heat is transferred through the bubble surface. Expressing the vapor mass flow rate and volumetric flow rate with  $q_I''$ :

$$\dot{m} = \frac{q_I''}{h} S \quad (12)$$

$$\dot{V} = \frac{q_I''}{h\rho_v} S \quad (13)$$

The evaporation results in a force due to the change in momentum as vapor pushes the bubble interface. Assuming that the force acts uniformly over the bubble surface, the velocity relative to the interface can be obtained by dividing volumetric flow rate by bubble surface area:

$$v = \frac{\dot{V}}{2\pi R^2 (1 + \cos \alpha)} \quad (14)$$

The resulting force due to the momentum change is given by the product of the evaporation mass flow rate and the vapor velocity relative to the interface:

$$F_{Mz} = \int_0^{2\pi} \int_0^{\pi-\alpha} \frac{1}{2\pi R^2 (1 + \cos \alpha)} \dot{m} v R^2 \sin \theta \, d\theta \, d\varphi \, \cos \theta \quad (15)$$

$$= -\frac{\pi}{2\rho_v} q_I''^2 (\cos 2\alpha - 1) \left[ \frac{S}{2\pi R h (\cos \alpha + 1)} \right]^2$$

The critical heat flux or CHF occurs when the force due to the momentum change  $F_M$  pushing the bubble interface into the liquid balances with the sum of the forces holding the bubble at the base. The bubble reaches the maximum radius at  $z$  direction at the CHF point, when given a small increment heat flux, the bubble will expand in the direction normal to  $z$  axis and combine with neighboring bubbles to form a vapor film over the heater surface. At the inception of the CHF condition, the force balance yields:

$$F_{Mz} + F_s \sin \alpha + F_{Pz} + F_G = 0 \quad (16)$$

Substituting equation (1)-(15) into (16), and make  $H = kR$  to simplify the equation, we can get the heat flux  $q_I''$ .  $X$  states the effect of adhesion force,  $Y$  means the effect of hydraulic pressure,  $Z$  means the effect of gravity:

$$q_I'' = K(X + \varphi Y + Z)^{\frac{1}{2}}$$

$$K = h\rho_v^{\frac{1}{2}} \pi^{\frac{1}{2}} \frac{1}{\sqrt{6}} \left[ \frac{\sigma g \sin^n \alpha}{(\rho_l - \rho_v)} \right]^{\frac{1}{4}}$$

$$X = \frac{24(\rho_l - \rho_v)}{\sin^n \alpha \pi^2}$$

$$Y = 3\rho_l(k - \cos \alpha) - 2\rho_l \frac{\cos^2 \alpha - \cos \alpha + 1}{(-\cos \alpha + 1)}$$

$$Z = \rho_v \frac{(\cos \alpha + 1)(-\cos \alpha + 2)}{(-\cos \alpha + 1)}$$

According to Kandlikar's CHF model, heat is removed by the bubble from an influence area as shown in Figure. 2, The heat flux on the heater surface is obtained:

$$q_{CHF} = q_I'' \left( \frac{1 + \cos \alpha}{16} \right)$$

Kandlikar's model did not take the effect of heater size on CHF value into consideration and is based on a circular heater with a diameter of 10 mm. Due to the heater size effect, CHF value on the bare surface does not agree with Kandlikar's prediction. As a result, a constant factor  $\Phi=0.7$  is multiplied with Kandlikar's

bare surface CHF prediction coefficient in accordance with the experimental data.

So the CHF value can be represented as:

$$q_{CHF} = K_{CHF}(X + \phi Y + Z)^{\frac{1}{2}} \quad (17)$$

Where

$$K_{CHF} = \Phi h \rho_v^{\frac{1}{2}} \frac{(\cos \alpha + 1) \pi^{\frac{1}{2}}}{16\sqrt{6}} \left[ \frac{\sigma g \sin^n \alpha}{(\rho_l - \rho_v)} \right]^{\frac{1}{4}}$$

Equation (17) predicts the CHF value for pool boiling of pure liquid over a smooth surface. It considers the combined effect of adhesion force, hydraulic pressure, and the effect of gravity. Both surface conditions as well as liquid properties are revealed in the correlation. This provides a basic correlation for further analysis on surface orientation and surface structures.

## 4. RESULTS AND DISCUSSIONS

### 4.1 Comparison between different models and experimental results

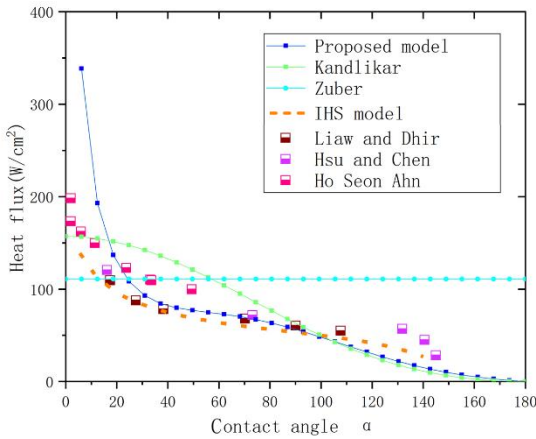


Figure. 4 Effect of contact angle on CHF for water boiling on a horizontal smooth surface.

In Figure 4, the Kandlikar model [9], Zuber model [5], IHS model [14] and the proposed model are compared with experimental data from Liaw and Dhir et al. [17], Hsu and Chen et al. [18], and Ho Seon Ahn et al. [19].

We can see that the proposed model predicts well at a wide range of contact angle with experimental data scattered around the curve. The CHF value reduces sharply when contact angle is near 0, and the decline is

moderate between around 20 and 100. When contact angle approaches 180, CHF value decreases to near 0.

According to Kandlikar's CHF correlation, there is almost no CHF enhancement when contact angle is below 10, but Kim and Kim [20] showed that with small contact angle, the CHF can be enhanced by the liquid spreading effect of capillary wicking. In the model proposed in this paper, when analyzing bubble behavior on a super hydrophilic surface, we can imagine that when the surface is highly wetted, the liquid spreading effect will be strong enough to cover the whole heater surface, so there will be no dry hot patch on the surface and CHF condition will never be reached. Theoretically, according to the proposed model, when dynamic contact angle reaches 0, the CHF value will be infinite large. Note that in this model, dynamic contact angle is used instead of contact angle, so there can be some error in terms of the predicted value and the experimental results. The dynamic contact angle will not be exact 0 under experimental conditions, so in experiments the infinite CHF will not be reached.

When contact angle reaches 180, it has been shown experimentally that CHF decreases to near-zero on non-wetting surfaces. This trend cannot be predicted using the IHS model, but can be expressed using the proposed model in this paper.

### 4.2 Effect of fluid properties

Figure 5 shows the CHF value change with contact angle on a smooth heating surface with different fluids: water, ethanol, and FC-72.

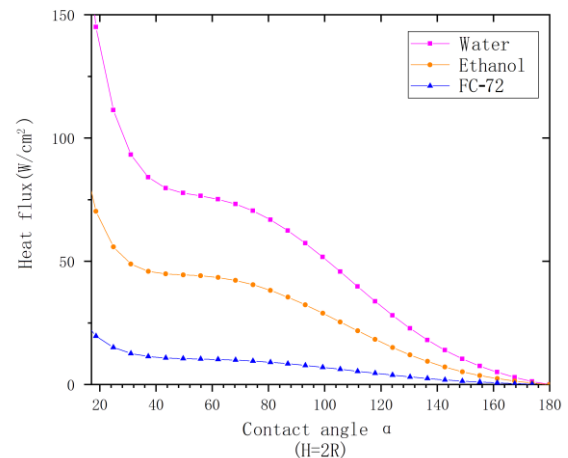


Figure. 5 Effects of contact angle on CHF and comparison of different fluids.

It is shown in Figure 5 that for different fluid properties, the CHF curve has the same trend of

decreasing with the increment of contact angle. The value of heat flux varies with different fluid medium (see Table 1 for physical properties of these fluids). That is because the bubble radius is largely affected by the density of the fluid. Also, the size of the bubble can affect the magnitude of the forces acting on the bubble. For water, ethanol, FC-72, the radius of the bubble at CHF point decreases, and the CHF value decreases along with the size of the bubble.

Table 1. Saturation properties of water, ethanol and FC-72 under the standard atmospheric pressure.

Fluids	$\rho_l$ ( $kg/m^3$ )	$\rho_v$ ( $kg/m^3$ )	$h_{fg}$ ( $J/kg$ )	$T_{sat}$ ( $K$ )	$\sigma_{lv}$ ( $N/m$ )
Water	958.4	0.5975	2257000	373	0.0589
Ethanol	789.45	1.56	855160	351.6	0.0154
FC-72	1680	13.4	94800	329	0.012

The small fluctuation of the curve is due to the effect of the hydraulic pressure. The magnitude of pressure is affected by the shape of the bubble. The bubbles in our analysis are assumed to be positively spherical, which is hard to be achieved in real boiling situations when contact angle is around 90. The curve can be further modified with bubble shape to better fit experimental observations.

#### 4.3 Effect of hydrostatic level

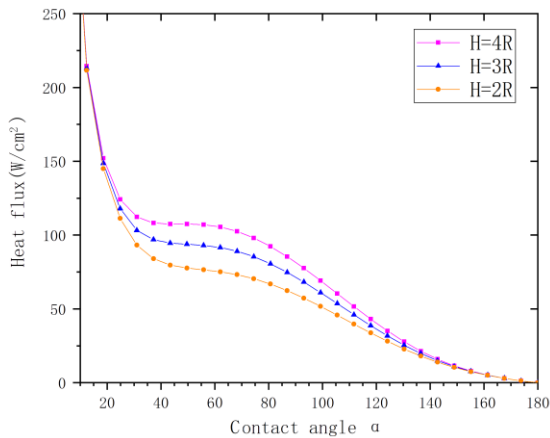


Figure. 6 Effects of hydrostatic level on CHF value with water as medium.

Figure 6 shows the change of heat flux with the change of contact angle at different liquid level height. It can be found that the value of CHF increases with the increase of the liquid level, and there is not much difference when the contact angle is near 0 and 180.

However, there are few experimental observations of liquid level influencing CHF reported in literature. This may be because when the liquid level is high, the turbulence in the chamber will be large and thus affect the visualization of the bubbles and the experimental results. So in current literature, pool boiling at a lower liquid level is always investigated. Most experiments study the surfaces with small contact angles, under that circumstance; the effect of liquid height is not obvious. And the correlation in this paper is consistent with the current experiments findings.

In the force balance analysis, it indicates that the bubble behavior can be affected by hydraulic pressure, the change in liquid height can affect the hydraulic pressure and thus affect the bubble shape and bubble behavior. This effect can be dominant when contact angle is around 90 according to the correlation. Because the bubble has the largest diameter in that condition, and the bubble is in a half sphere shape, which can be most affected by hydraulic pressure. However, little experimental evidence has been found regarding liquid height with surface contact angle around 90. Experiments can be done on this to further explore the influence parameters on CHF value in the future.

#### 4.4 Effect of surface geometry

The presence of micro/nano structures can affect the liquid rewetting phenomenon, and thereby postpone the dry out phenomenon occurring at the CHF point and significantly enhance the CHF value. Furthermore, micro/nanostructures can significantly influence the thermal conductivity, solid-liquid adhesion force, capillary wicking, and Rayleigh-Taylor instability wavelength, judging from previous studies.

The CHF model in this paper can be further modified to be applied to micro scale structures, especially microstructure with fins at the magnitude of  $\mu m$ , which means that the fin upper surface area is much smaller than the bubble base area. The correlation can be modified by changing the adhesion force and hydraulic pressure term to fit the condition of a micro structured surface.

## 5. CONCLUSIONS

This model referred to Kandlikar's CHF model, uses three-dimensional force balance to achieve a theoretical model for critical heat flux on a heated surface. Critical wavelengths of Taylor instability is considered on a smooth surface with different contact angle and liquid properties. Effects of capillary wicking

force, gravity, evaporation, and hydraulic pressure are taken into consideration simultaneously in this model. It can be concluded from the present paper that:

(1) Among the effect of different forces, the effect of hydraulic pressure is the most dominant one. As it affects the bubble departure behavior and bubble shape.

(2) Higher surface wettability (smaller liquid contact angle) contributes to higher CHF value. Improving the dynamic contact angle of the surface can largely enhance the CHF value. Also, surface structures that can assist the collapse of bubbles near the surface and generate more nuclei bubbles can improve the bubble departure performance, thus leads to higher CHF value.

(3) The influence of liquid height over CHF value is not obvious with contact angle around 0 and 180. The condition of contact angle at around 90 can be further analyzed based on more experimental observations.

(4) The CHF values obtained from this model are in agreement with existing experimental data for pool boiling for different fluids and contact angles within a wide range. Thus, further analysis of surface orientation and micro structures can be conducted based on this model by modifying the capillary force factor and hydraulic pressure factor.

## REFERENCE

[1] Ali Radwan, Shinichi Ookawara, Shinsuke Mori, Mahmoud Ahmed, Uniform cooling for concentrator photovoltaic cells and electronic chips by forced convective boiling in 3D-printed monolithic double-layer microchannel heat sink, *Energy Conversion and Management* 166 (2018) 356-371.

[2] Shoukat Alim Khan, Nurettin Sezer, Salman Ismail, Muammer Koç, Design, synthesis and nucleate boiling performance assessment of hybrid micro-nano porous surfaces for thermal management of concentrated photovoltaics (CPV), *Energy Conversion and Management* 195 (2019) 1056-1066.

[3] Maan Al-Zareer, Ibrahim Dincer, Marc A. Rosen, Novel thermal management system using boiling cooling for highpowered lithium-ion battery packs for hybrid electric vehicles, *Journal of Power Sources* 363 (2017) 291-303.

[4] Kutateladze, S.S. , 1950. Hydromechanical model of heat transfer crisis in pool liquid boiling. *J. Tech. Phys.* 20 (11).

[5] Zuber, N. , 1959. Hydrodynamic Aspects Of Boiling Heat Transfer (Thesis). United States Atomic Energy Commission.

[6] Lienhard, H. , Dhir, V.K. , Riherd, D. , 1973. Peak pool boiling heat -flux measurements on finite horizontal flat plates. *J. Heat Transf.* (November) 477–482.

[7] Yagov, V.V. , 2014. Is a crisis in pool boiling actually a hydrodynamic phenomenon? *Int. J. Heat Mass Tran.* 73, 265–273 Elsevier Ltd.

[8] Fang, X. , Dong, A. , 2016. A comparative study of correlations of critical heat flux of pool boiling. *Journal of Nuclear Science and Technology* 3131 (July), 1–12.

[9] Kandlikar, S.G. , 2001. A Theoretical Model to Predict Pool Boiling CHF Incorporating Effects of Contact Angle and Orientation. *J. Heat Transf.* 123 (6), 1071.

[10] Haramura, Y. , Katto, Y. , 1983. A new hydrodynamic model of critical heat flux, applicable widely to both pool and forced convection boiling on submerged bodies in saturated liquids. *Int. J. Heat Mass Tran.* 26 (3), 389–399.

[11] Chu, I.C. , et al., 2014. Observation of critical heat flux mechanism in horizontal pool boiling of saturated water. *Nucl. Eng. Des.* 279, 189–199.

[12] Chu, I.C. , No, H.C. , Song, C.H., 2013. Visualization of boiling structure and critical heat flux phenomenon for a narrow heating surface in a horizontal pool of saturated water. *Int. J. Heat Mass Tran.* 62 (1), 142–152.

[13] Yagov, V.V. , 1988. A physical model and calculation formula for critical heat fluxes with nucleate pool boiling of liquids. *Therm. Eng.* 35.

[14] Huayong Zhao, Andrew Williams, Predicting the critical heat flux in pool boiling based on hydrodynamic instability induced irreversible hot spots, *International Journal of Multiphase Flow* 104 (2018) 174–187.

[15] C.P. Costello, W.J. Frea, The roles of capillary wicking and surface deposits in the attainment of high pool boiling burnout heat fluxes, *AIChE J.* 10 (1965) 393–398.

[16] R.W.L. Fong, T. Nithenandan, C.D. Bullock, L.F. Slater, G.A. McRae, Effect of oxidation and fractal surface roughness on the wettability and critical heat flux of glass-peened zirconium alloy tubes, in: *Proceedings of the Fifth International Conference on Boiling Heat Transfer*, 2003.

[17] Liaw, S.P., Dhir, V.K., 1986. Effect of surface wettability on transition boiling heat transfer from a vertical surface. In: *Proceedings of the 8th International Heat and Mass Transfer*, 4, pp. 2031–2036.

[18] Hsu, C.-C. , Chen, P.-H. , 2012. Surface Wettability Effects on Critical Heat Flux of Boiling Heat Transfer using Nanoparticle Coatings. *Int. J. Heat Mass Tran.* 55(13–14), 3713–3719.

[19] Ho Seon Ahn, Hang Jin Jo, Soon Ho Kang, and Moo Hwan Kim, Effect of liquid spreading due to nano/microstructures on the critical heat flux during pool boiling, *Appl. Phys. Lett.* 98, 071908 (2011).

[20] H. Kim, M.H. Kim, Effect of nanoparticle deposition on capillary wicking that influences the critical heat flux in nanofluids, *Appl. Phys. Lett.* 91 (2007) 014104.